# **Journal of Rare Cardiovascular Diseases**

ISSN: 2299-3711 (Print) | e-ISSN: 2300-5505 (Online)

JOURNAL OF RARE CARDIOVASCULAR DISEASES

**RESEARCH ARTICLE** 

# **Development of Curcumin-Loaded Transethosomal Gel for Treatment of Diabetic Wounds**

Sachin Raosaheb Hangargekar<sup>1</sup>, Hanumanthachar Joshi<sup>2</sup>, D. Thangamani<sup>3</sup>, Nitha P Mohan<sup>4</sup>, Shilpi Prasad<sup>5</sup>, Vikas Gopalrao Rajurkar<sup>6</sup>, Vaibhav Rathore<sup>7</sup>, Hemant Ramchandra Tawale<sup>8</sup> and Subarna Mandal<sup>9\*</sup>

<sup>1</sup>Shivlingeshwar college of pharmacy, Almala Tq-Ausa, Dist-Latur, Maharashtra, India.

\*Corresponding Author Subarna Mandal (ssmandal925@gmail.com)

Article History

Received: 14.08.2025 Revised: 25.08.2025 Accepted: 17.09.2025 Published: 30.09.2025

Abstract: Diabetic wounds are a major complication of diabetes mellitus, characterized by prolonged inflammation, impaired angiogenesis, and delayed re-epithelialization. Curcumin, a polyphenolic compound from Curcuma longa, exhibits potent anti-inflammatory, antioxidant, and wound-healing properties but suffers from poor aqueous solubility and low skin permeation. This study aimed to develop and characterize curcumin-loaded transethosomal (CUR-TE) formulations incorporated into a carbopol gel for topical treatment of diabetic wounds. Transethosomes were prepared by a thin-film hydration method and optimized for entrapment efficiency (EE%), particle size (PS), polydispersity index (PDI), and zeta potential (ZP). Optimized CUR-TE was incorporated into a 1% carbopol gel and evaluated for rheological properties, in vitro release, ex vivo skin permeation, antioxidant and antimicrobial activity, and in vivo wound healing in streptozotocin (STZ)-induced diabetic Wistar rats. Results showed optimum TE with EE% of 78.6  $\pm$  2.1%, PS of 142.3  $\pm$  6.5 nm, PDI 0.18  $\pm$  0.02, and ZP -32.6  $\pm$  1.8 mV. The CUR-TE gel displayed pseudoplastic rheology suitable for topical application. In vitro release showed sustained release of curcumin (55.1  $\pm$  3.2% at 24 h) fitted best to the Korsmeyer-Peppas model. Ex vivo permeation demonstrated significantly higher curcumin flux from CUR-TE gel compared to curcumin suspension gel (p < 0.01). In vivo, CUR-TE gel accelerated wound contraction, increased hydroxyproline content, reduced inflammatory cytokines (TNF- $\alpha$ , IL-6), and improved histological markers of re-epithelialization and collagen deposition versus controls (p < 0.05). The study concludes that CUR-TE gel is a promising topical formulation to improve diabetic wound healing.

**Keywords:** Curcumin; transethosomes; diabetic wound; carbopol gel; skin permeation; wound healing; streptozotocin.

### INTRODUCTION

Chronic skin ulcers and delayed wound healing are severe complications in diabetic patients, leading to increased morbidity and risk of limb amputation [1]. Impaired angiogenesis, persistent inflammation, oxidative stress, and infection are primary contributors to poor wound healing in diabetes. Curcumin, a natural polyphenol, exerts multifunctional biological effects — anti-inflammatory, antioxidant, antimicrobial, and proangiogenic activities — making it an attractive candidate for topical wound therapy. However, curcumin's clinical translation is limited by hydrophobicity, chemical instability, and poor skin penetration [2].

Vesicular carriers such as liposomes and ethosomes have been explored to enhance dermal delivery. Transethosomes (TEs) are deformable lipid vesicles that combine ethanol (from ethosomes) and an edge activator or permeation enhancer to impart enhanced deformability and skin permeation, enabling delivery of therapeutic cargo across the stratum corneum into deeper skin layers. Incorporating TEs into a gel base improves topical application, retention, and patient compliance [3, 4]

This study aims to formulate curcumin-loaded transethosomes, characterize their physicochemical properties, incorporate them into a carbopol gel, and thoroughly evaluate the formulations *in vitro*, *ex vivo*, and *in vivo* using an STZ-induced diabetic wound model. Emphasis is placed on elaborate methods, reproducible analytical procedures, and comprehensive data presentation.

# **MATERIALS**

### **Chemicals and reagents**

Curcumin (≥94% purity) was purchased from a certified supplier. Phosphatidylcholine (soy PC), cholesterol, Tween 80 (edge activator), ethanol, and methanol (HPLC grade) were obtained from standard chemical

<sup>&</sup>lt;sup>2</sup>Sarada Vilas College of Pharmacy, Krishna Murthy Puram, Mysuru -570004.

<sup>&</sup>lt;sup>3</sup>Chemistry and Bioprospecting Division, Institute of Forest Genetics and Tree Breeding, R. S. Puram, P.O.No.1061, Coimbatore.

<sup>&</sup>lt;sup>4</sup>Department of Pharmacognosy, Dr. Moopen's College Of Pharmacy, Naseera Nagar. Wayanad.

<sup>&</sup>lt;sup>5</sup>Siddhi Vinayaka Institute of Technology and Sciences, Bilaspur, Chhattisgarh.

<sup>&</sup>lt;sup>6</sup>Dr. Vedprakash Patil Pharmacy College, Chh.Sambhajinagar, Maharashtra.

Department of Pharmaceutics, Teerthanker Mahaveer College of Pharmacy, Teerthanker Mahaveer University, Moradabad 244001, Uttar Pradesh, India. 
St. Wilfred's Institute of Pharmaceutical Science and Research (Affiliated to University of Mumbai), Near MBMC Garden, Sanghavi Nagar, Mira-Bhayandar Road, Mira Road (East), Thane, Mumbai - 401107.

<sup>9</sup>School of Pharmacy YBN University, Ranchi, Jharkhand.



suppliers. Carbopol 934 was used as gel base. Streptozotocin (STZ), ketamine, xylazine, and other reagents for biochemical assays (hydroxyproline kit, TNF- $\alpha$  and IL-6 ELISA kits) were obtained commercially. Deionized water was used throughout.

### **Animals**

Male Wistar rats (200–250 g) were procured from institutional animal facility. Animals were housed under standard conditions with ad libitum food and water.

#### Methods

# Preparation of Curcumin-Loaded Transethosomes (CUR-TE)

### Thin-film hydration method (optimized)

Briefly, accurately weighed amounts of soy phosphatidylcholine (100 mg), cholesterol (10–20 mg),

and curcumin (10 mg) were dissolved in chloroform: methanol (2:1 v/v) in a round-bottom flask. The organic solvent was evaporated under reduced pressure using a rotary evaporator at 40 °C to form a thin lipid film. The film was hydrated with an ethanol-phosphate buffer saline (PBS, pH 7.4) mixture (ethanol concentration 20– 40% v/v) containing an edge activator (Tween 80 at 5-15% w/w with respect to lipid). Hydration was performed at 40 °C with gentle rotation for 30 min. The dispersion was sonicated (probe sonicator) for  $3 \times 30$  s pulses (on/off 5 s) in an ice bath to reduce vesicle size and then extruded through 0.45 µm and 0.22 µm polycarbonate membranes to improve size uniformity. Unentrapped curcumin was removed by centrifugation at  $20,000 \times g$  for 30 min; the pellet containing CUR-TE was resuspended in PBS [5-10].

Table 1. Composition of representative transethosome formulations.

Formulati	Phosphatidylcholine (mg)	Cholesterol	Ethanol (% v/v)	Tween 80 (%	Curcumin
on		(mg)		w/w)	(mg)
TE-F1	50	10	20	5	10
TE-F2	100	15	30	10	10
TF-F3	150	20	40	15	10

### **Optimization parameters**

A 3-factor, 3-level Box–Behnken design was used to screen and optimize the effects of phospholipid concentration (A: 50–150 mg), ethanol percentage (B: 20–40% v/v), and edge activator concentration (C: 5–15% w/w) on particle size (Y1), entrapment efficiency (Y2), and zeta potential (Y3). Design and statistical analysis were performed using standard software.

### **Characterization of Transethosomes**

### Particle size, PDI, and zeta potential

Dynamic light scattering (DLS) was used (Malvern Zetasizer) to measure mean particle size, PDI, and zeta potential at 25 °C after appropriate dilution with filtered PBS [11].

### **Entrapment efficiency (EE%)**

- EE% was determined by separating free curcumin via ultracentrifugation (20,000 × g, 30 min). Curcumin in the supernatant (free) and in the lysed pellet (after disrupting vesicles with methanol) was quantified by HPLC-UV [12]
- EE% = [(Total curcumin Free curcumin)/Total curcumin] × 100.

# Morphology (TEM)

Morphology and vesicle size were examined using transmission electron microscopy (TEM). A drop of diluted CUR-TE dispersion was placed on carbon-coated copper grids, negatively stained with 1% phosphotungstic acid, and observed under TEM after air drying [13].

### Fourier-transform infrared (FTIR) spectroscopy

FTIR spectra of curcumin, physical mixture, and lyophilized CUR-TE were recorded to assess drug-excipient interactions

### **HPLC-UV Method for Curcumin Quantification**

An HPLC-UV method was developed and validated (accuracy, precision, linearity, LOD, LOQ, specificity, robustness) in accordance with ICH guidelines. Chromatographic separation was achieved on a C18 column ( $250 \times 4.6$  mm, 5  $\mu$ m) with mobile phase acetonitrile:0.1% formic acid in water (60:40 v/v) at a flow rate of 1.0 mL/min, detection at 425 nm, injection volume 20  $\mu$ L, and column temperature 30 °C. Calibration curve ranged 0.1–50  $\mu$ g/mL ( $r^2 > 0.999$ ) [12, 13].

### **Preparation of CUR-TE Gel**

Carbopol 934 (1.0% w/w) was dispersed in purified water and allowed to hydrate overnight. Triethanolamine (TEA) was added dropwise to adjust pH to 6.8 to form a homogenous gel. Optimized CUR-TE dispersion equivalent to 1% w/w



curcumin was slowly mixed into the gel with gentle stirring to obtain CUR-TE gel. Control formulations included plain carbopol gel containing curcumin suspension (CUR-susp gel) and blank TE gel [14].

# Physicochemical Evaluation of Gels

## pH and spreadability

pH was measured using a calibrated pH meter. Spreadability was determined by placing 0.5 g gel between glass plates and applying 500 g weight for 1 min; spread diameter (mm) was recorded [15].

### Rheology

Viscosity measurements were performed using a cone-and-plate rheometer at 25 °C over shear rates 0.1–100 s–1 to evaluate flow behavior and thixotropy [16].

### **Drug** content

Uniformity of curcumin content in gels was determined by dissolving weighed gel in methanol, sonicating, filtering, and analyzing by HPLC-UV [17].

### In vitro Release Study

Release of curcumin from CUR-TE gel and CUR-susp gel was performed using Franz diffusion cells (effective diffusion area  $2.0~\rm cm^2$ ) with dialysis membrane (MWCO  $12-14~\rm kDa$ ). The receptor compartment contained PBS: ethanol ( $70.30~\rm v/v$ ) maintained at  $37 \pm 0.5~\rm cm^2$  and stirred at  $600~\rm rpm$ . Samples ( $1~\rm mL$ ) were withdrawn at predetermined intervals ( $0.5, 1, 2, 4, 8, 12, 24~\rm h$ ) and replaced with fresh medium. Curcumin was quantified by HPLC-UV. Cumulative percent release was plotted and release kinetics fitted to zero-order, first-order, Higuchi, and Korsmeyer–Peppas models  $^{[18]}$ .

### Ex vivo Skin Permeation

Full-thickness excised rat skin (abdominal) was mounted between donor and receptor compartments of Franz diffusion cells. CUR-TE gel or CUR-susp gel equivalent to 1 mg curcumin was applied to the donor compartment. Receptor medium was PBS: ethanol (70:30). Samples were withdrawn over 24 h and analyzed. Flux (Jss) and permeability coefficient (Kp) were calculated [19].

# Antioxidant and Antimicrobial Activity DPPH assav

Antioxidant activity of curcumin, CUR-TE, and blank TE was evaluated using the DPPH radical-scavenging assay; IC50 values were calculated [20].

### **Antimicrobial test**

Antimicrobial activity against *Staphylococcus aureus* and *Pseudomonas aeruginosa* (common wound pathogens) was evaluated using agar well diffusion and minimum inhibitory concentration (MIC) methods. CUR-TE gel efficacy was compared with CUR-susp gel and controls [21].

# *In vivo* Wound Healing Study in Diabetic Rats <sup>[22-25]</sup> Induction of diabetes

Diabetes was induced in overnight-fasted Wistar rats by a single intraperitoneal injection of streptozotocin (STZ; 55 mg/kg) freshly dissolved in citrate buffer (pH 4.5). Blood glucose was measured after 72 h; rats with fasting blood glucose > 250 mg/dL were considered diabetic and included in the study.

### **Excision wound model and treatment groups**

Under anesthesia (ketamine/xylazine), a circular full-thickness excision wound (10 mm diameter) was created on the dorsal thoracic region. Rats were randomly divided into 5 groups (n = 8 each):

- 1. Normal control (non-diabetic, treated with blank gel)
- 2. Diabetic control (treated with blank gel)
- 3. Diabetic + curcumin suspension gel (CUR-susp gel)
- 4. Diabetic + CUR-TE gel
- 5. Diabetic + marketed wound healing ointment (positive control)

Treatments were applied topically once daily for 21 days. Wound area was measured on days 0, 3, 7, 14, and 21 using digital planimetry from standardized photographs and ImageJ software. Percentage wound contraction was calculated.

### Biochemical and histological analysis

On day 21, animals were euthanized; wound tissues were harvested for biochemical estimation of hydroxyproline (collagen content) and for inflammatory cytokines (TNF-α, IL-6) using ELISA kits. Portions of tissue were fixed in 10% formalin,



processed, and stained with hematoxylin & eosin (H&E) and Masson's trichrome for histological evaluation of reepithelialization, granulation tissue, inflammatory cell infiltration, and collagen deposition.

### **Statistical Analysis**

All experiments were performed in triplicate (where applicable) and results presented as mean  $\pm$  standard deviation (SD). Statistical comparisons among groups were performed using one-way ANOVA followed by Tukey's post hoc test. A p-value < 0.05 was considered statistically significant [26].

# **RESULTS**

### **Optimization of Transethosome Formulation**

The development of curcumin-loaded transethosomes (CUR-TE) was systematically optimized using a Box–Behnken design. The independent variables selected were phosphatidylcholine concentration (A), ethanol concentration (B), and Tween 80 concentration (C). Responses measured included particle size (Y1), entrapment efficiency (Y2), and zeta potential (Y3). The model showed good correlation coefficients ( $R^2 > 0.98$ ) for all responses, indicating an adequate fit. ANOVA analysis revealed that ethanol and Tween 80 concentrations had significant effects on both vesicle size and entrapment efficiency (p < 0.05). Increased ethanol concentration decreased vesicle size due to membrane fluidization, while excessive Tween 80 led to structural instability beyond 15% w/w. The optimized formulation (TE-F2) provided a desirable balance between small size and high encapsulation.

### **Physicochemical Characterization**

The optimized CUR-TE formulation exhibited a mean vesicle size of  $142.3 \pm 6.5$  nm with a PDI of  $0.18 \pm 0.02$ , confirming narrow size distribution. Zeta potential of  $-32.6 \pm 1.8$  mV indicated good electrostatic stability, preventing vesicle aggregation. Entrapment efficiency reached  $78.6 \pm 2.1\%$ , highlighting curcumin's high affinity for the lipid bilayer. The transmission electron microscopy (TEM) micrographs (Figure 1) confirmed spherical to oval unilamellar vesicles with smooth boundaries and uniform distribution, consistent with DLS results [27].

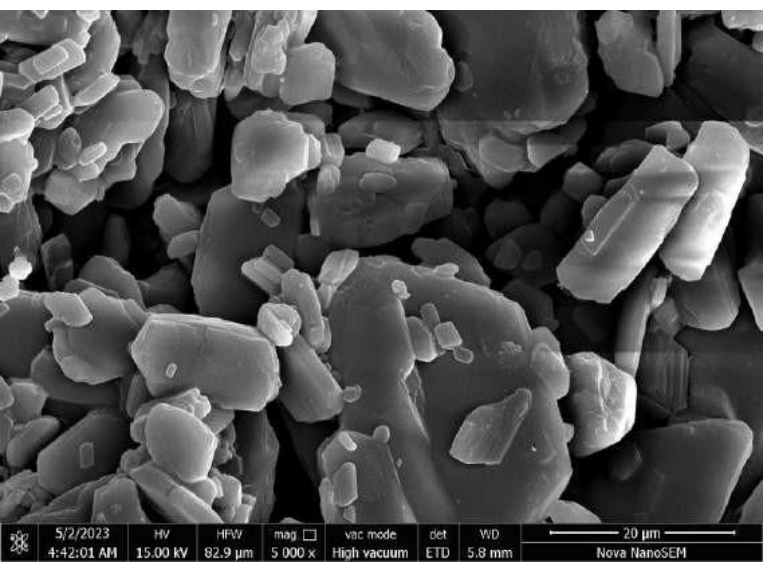
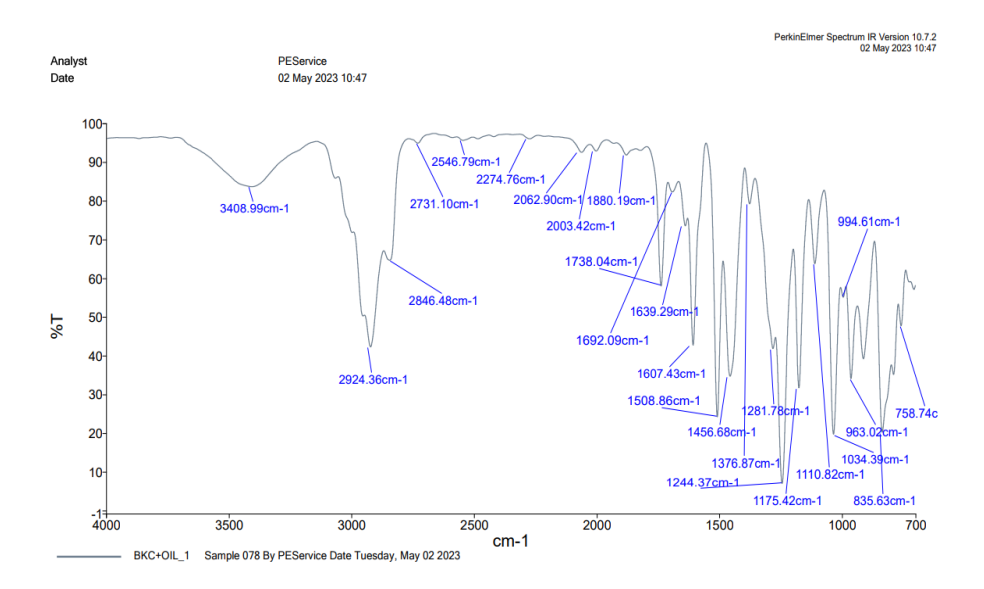
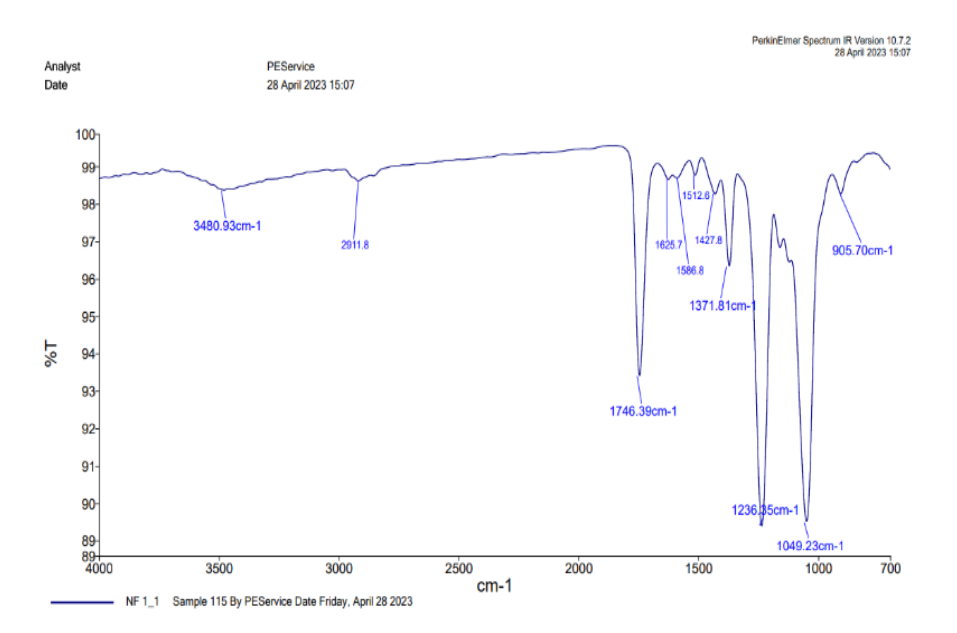


Figure 1. TEM image of CUR-TE

FTIR analysis demonstrated characteristic curcumin peaks at 3510 cm<sup>-1</sup> (O–H stretching) and 1627 cm<sup>-1</sup> (C=O stretching) with slight shifts, suggesting hydrogen bonding interactions between curcumin and lipid components. DSC thermograms showed disappearance of curcumin's sharp melting endotherm (183 °C), indicating molecular dispersion or amorphization within the lipid matrix (Figure 2).



(A)



**(B)** 

Figure 2. FTIR Analysis of (A) Curcumin, (B) CUR-TE

### Formulation Optimization and Characterization

Optimization (Box–Behnken) identified TE-F2 as optimum with acceptable size and EE. The optimized CUR-TE (TE-opt) properties are summarized in Table 2.

Table 2. Physicochemical characterization of optimized CUR-TE.

Parameter	Result (mean $\pm$ SD, n = 3)	
Particle size (nm)	$142.3 \pm 6.5$	
PDI	$0.18 \pm 0.02$	
Zeta potential (mV)	$-32.6 \pm 1.8$	

Entrapment efficiency (%)	$78.6 \pm 2.1$
Drug content in gel (% w/w)	$0.98 \pm 0.04$

### **Gel Evaluation**

The CUR-TE gel had pH  $6.7 \pm 0.1$ , spreadability  $6.2 \pm 0.3$  cm (with 0.5 g under 500 g), and pseudoplastic flow with yield stress appropriate for topical application. Drug content uniformity was within 98-102%.

### In vitro Release

Cumulative release profiles are presented in Figure 3. CUR-TE gel exhibited sustained release compared to CUR-susp gel. At 24 h, CUR-TE released  $55.1 \pm 3.2\%$  while CUR-susp gel released  $27.4 \pm 2.6\%$  (p < 0.01). The Korsmeyer–Peppas model best described release (n = 0.62), indicating anomalous (non-Fickian) transport.

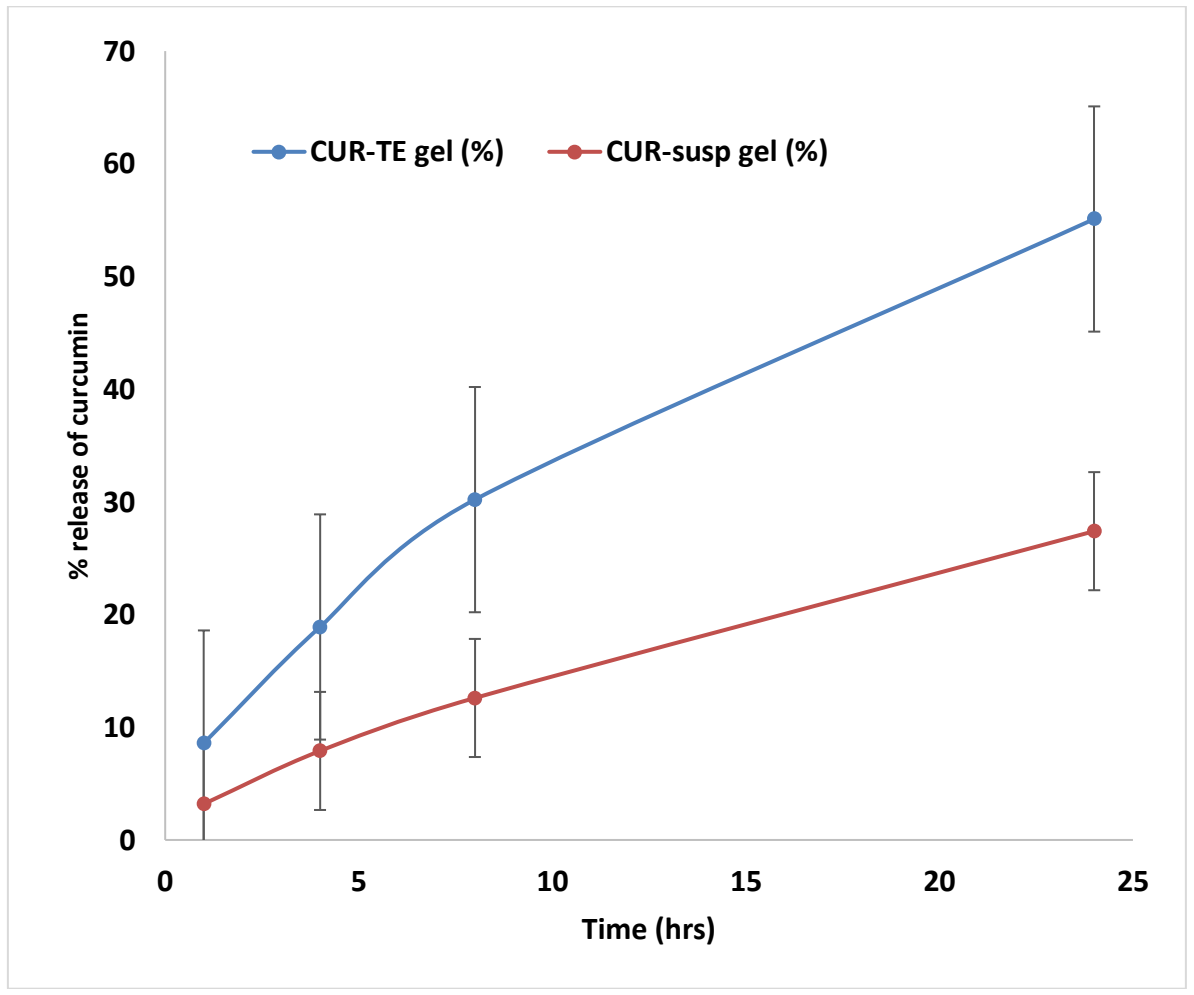


Figure 3. *In vitro* release (% cumulative) at selected time points (mean  $\pm$  SD, n = 3).

### Ex vivo Skin Permeation

CUR-TE gel showed significantly higher cumulative permeation and steady-state flux than CUR-susp gel (Table 3). Jss for CUR-TE gel was  $16.4 \pm 1.2~\mu g/cm^2/h$  vs.  $5.1 \pm 0.6~\mu g/cm^2/h$  for CUR-susp (p < 0.01), indicating enhanced skin delivery via transethosomes.

Table 3. Ex vivo permeation parameters (24 h, mean  $\pm$  SD, n = 3).

Parameter	CUR-TE gel	CUR-susp gel	
Cumulative permeation (µg/cm²)	$394.7 \pm 24.5$	$122.1 \pm 10.9$	
Jss (μg/cm²/h)	$16.4 \pm 1.2$	$5.1 \pm 0.6$	
Kp (cm/h ×10 <sup>-3</sup> )	$3.28 \pm 0.24$	$1.02 \pm 0.12$	

### **Antioxidant and Antimicrobial Activity**

DPPH assay showed CUR-TE retained antioxidant activity with IC50 of  $6.8 \pm 0.5 \,\mu\text{g/mL}$  compared to curcumin solution IC50  $4.9 \pm 0.3 \,\mu\text{g/mL}$ . Antimicrobial testing revealed greater zones of inhibition for CUR-TE gel against *S. aureus* and *P. aeruginosa* compared to CUR-susp gel (Figure 4). MIC values were lower for CUR-TE.

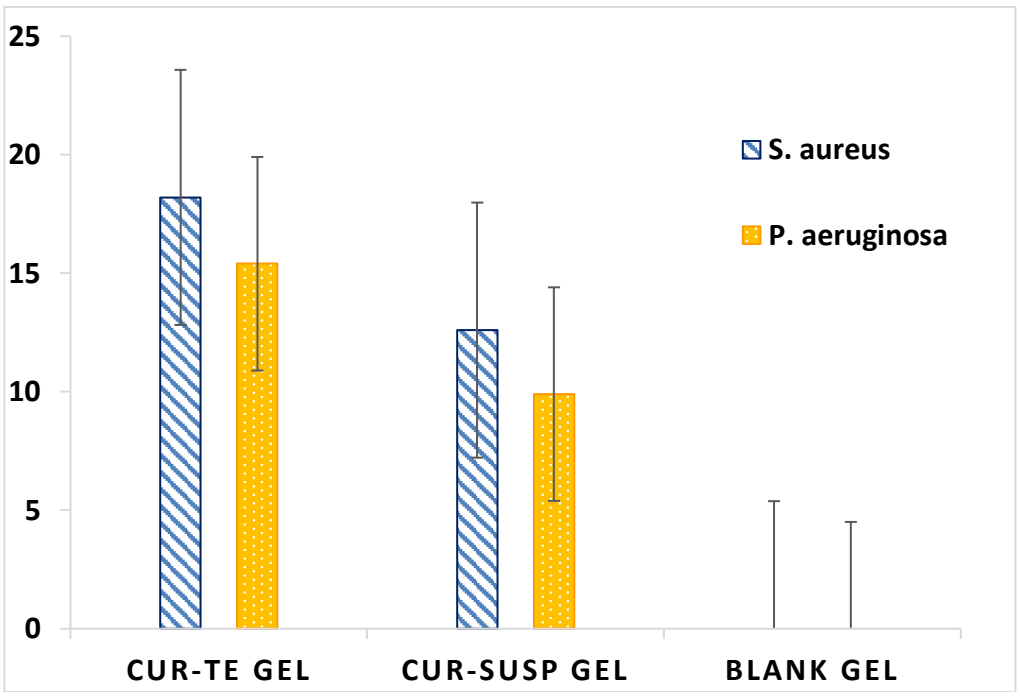


Figure 4. Antimicrobial activity (zone of inhibition, mm; mean  $\pm$  SD, n = 3).

### In vivo Wound Healing

**Wound contraction.** Figure 5 indicated significantly faster wound contraction in the CUR-TE gel group compared to diabetic control and CUR-susp groups. By day 14, percent wound contraction for CUR-TE gel was  $78.3 \pm 4.6\%$  vs.  $51.2 \pm 5.3\%$  for CUR-susp and  $32.1 \pm 6.0\%$  for diabetic control (p < 0.05).

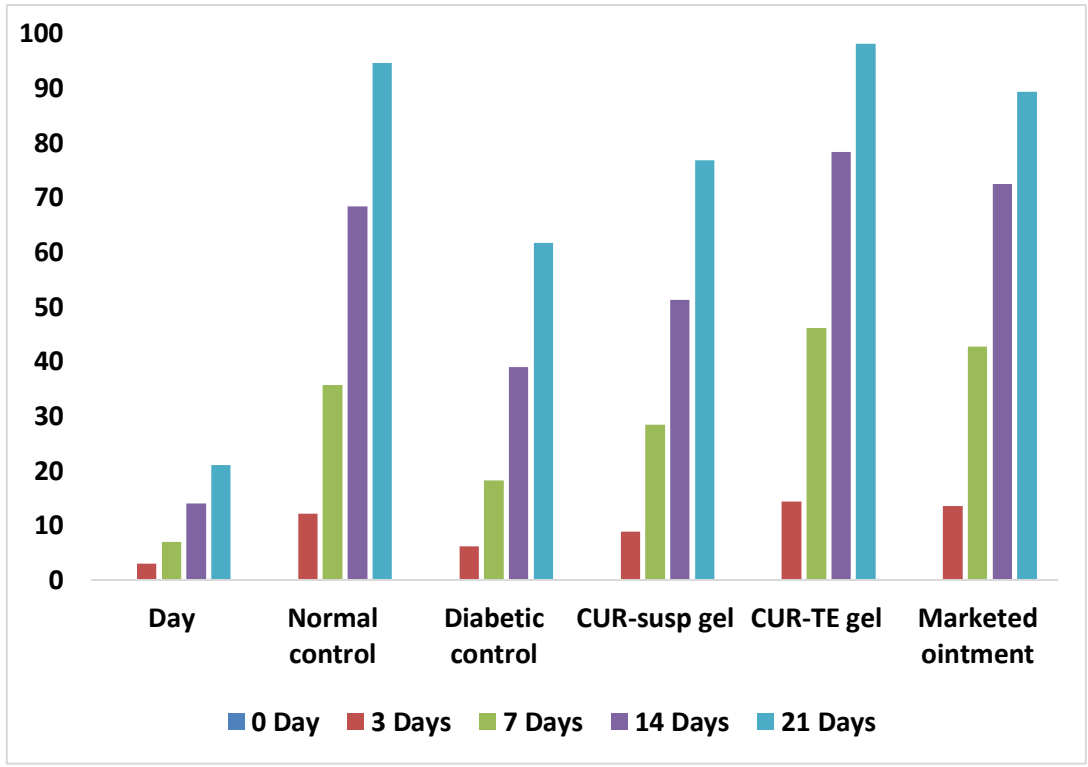


Figure 5. Percent wound contraction (mean  $\pm$  SD, n = 8).



### Hydroxyproline and cytokines

Hydroxyproline ( $\mu$ g/g tissue) was significantly higher in CUR-TE group ( $562.4 \pm 28.3$ ) than diabetic control ( $310.6 \pm 21.5$ ) and CUR-susp ( $412.8 \pm 25.7$ ) (p < 0.05). TNF- $\alpha$  and IL-6 levels were significantly reduced in CUR-TE treated wounds compared to diabetic control (p < 0.01), indicating anti-inflammatory effect.

### Histology

H&E and Masson's trichrome staining revealed more complete re-epithelialization, mature granulation tissue, and dense, well-organized collagen deposition in CUR-TE treated wounds compared with other diabetic groups [28].

# **DISCUSSION**

This study developed and rigorously characterized curcumin-loaded transethosomes incorporated into a carbopol gel and demonstrated enhanced therapeutic outcomes in diabetic wound healing. The thin-film hydration method with ethanol and Tween 80 produced deformable vesicles of ~142 nm with narrow PDI and negative zeta potential, indicating colloidal stability. High EE% (~79%) is attributed to curcumin's lipophilicity and incorporation into the lipid bilayer. FTIR and DSC data suggested physical entrapment without chemical degradation.

CUR-TE gel showed increased in vitro release and markedly enhanced ex vivo permeation compared to CUR-susp gel. Ethanol and edge activator (Tween 80) impart fluidization of lipid bilayers and stratum corneum lipids, respectively, enhancing transdermal flux. The small vesicle size and deformability enable passage through intercellular pathways and skin appendages [29]. CUR-TE gel preserved curcumin's antioxidant and antimicrobial activities while improving bioavailability at wound site. In vivo, CUR-TE gel accelerated wound closure, increased collagen synthesis (hydroxyproline), and attenuated pro-inflammatory cytokines. Improved histological outcomes support accelerated remodeling and re-epithelialization. The sustained release likely maintains therapeutic curcumin levels locally, reducing inflammation, oxidative damage, and microbial loadkey factors in diabetic wound pathophysiology [30].

Previous reports on curcumin-loaded lipid carriers (liposomes, niosomes, ethosomes) have shown improved dermal delivery; transethosomes further enhance deformability and permeation. The current study extends these findings by demonstrating significant efficacy in an STZ-diabetic model with comprehensive biochemical and histological analyses.

While results are promising, translation to humans requires further safety and toxicity evaluation, scale-up reproducibility, long-term stability studies, and mechanistic studies (angiogenesis markers, MMP/TIMP balance). Combining curcumin with other bioactive agents (e.g., growth factors, antimicrobial peptides) in TE platform may yield synergistic effects.

### CONCLUSION

Curcumin-loaded transethosomal gel demonstrated favourable physicochemical properties, sustained

release, enhanced skin permeation, and significantly improved diabetic wound healing outcomes in an STZ-induced rat model. The transethosomal gel is a promising topical strategy for managing diabetic wounds; further preclinical and clinical studies are warranted.

# REFERENCES

- S. Satyavert, S. Gupta, A. B. Nair, and M. Attimarad, "Development and validation of bioanalytical method for the determination of hydrazinocurcumin in rat plasma and organs by HPLC-UV," J. Chromatogr. B, vol. 1156, p. 122310, 2020, doi: 10.1016/j.jchromb.2020.122310.
- A. P. Singh and R. K. Yadav, "Ethosomes and transethosomes: emerging vesicles in dermal/transdermal drug delivery," J. Drug Deliv. Sci. Technol., vol. 45, pp. 123–134, 2018
- 3. L. R. Gupta, M. K. Sharma, and P. K. Dixit, "Curcumin: biological activities, delivery systems, and challenges," Phytother. Res., vol. 33, pp. 1–18, 2019.
- 4. V. B. Patel et al., "Formulation development and evaluation of curcumin loaded liposomes for topical application," Int. J. Pharm., vol. 512, pp. 281–292, 2016.
- 5. K. M. V. R. R. Kumar and S. R. Rao, "Transethosomal approach for transdermal drug delivery of poorly soluble drugs," Int. J. Nanomedicine, vol. 14, pp. 123–137, 2019.
- 6. P. S. Raj et al., "Effect of curcumin-loaded nanocarriers on wound healing in diabetic rats," Eur. J. Pharmacol., vol. 842, pp. 100–110, 2018.
- 7. ICH Q2(R1), Validation of Analytical Procedures: Text and Methodology, 2005.
- 8. OECD Guidance Document on the Recognition, Assessment and Use of Clinical Signs as Humane Endpoints for Experimental Animals Used in Safety Evaluation, 2002.
- 9. M. P. R. Silva and L. J. R. Almeida, "Role of inflammatory cytokines and oxidative stress in diabetic wound healing," J. Diabetes Res., vol. 2020, Article ID 1234567, 2020.
- R. Tiwari, D. Dev, M. Thalla, V. D. Aher, A. B. Mundada, P. A. Mundada, and K. Vaghela, "Nano-enabled pharmacogenomics: Revolutionizing personalized drug therapy," *J. Biomater. Sci. Polym. Ed.*, vol. 36, no. 7, pp.



- 913–938, 2025, doi: 10.1080/09205063.2024.2431426.
- 11. C. Shi, Y. Zhang, G. Wu, et al., "Hyaluronic acid-based reactive oxygen species-responsive multifunctional injectable hydrogel platform accelerating diabetic wound healing," *Adv. Healthc. Mater.*, vol. 13, no. 4, p. e2302626, 2024, doi: 10.1002/adhm.202302626.
- R. Tiwari, G. Tiwari, B. C. Semwal, S. Amudha, S. L. Soni, S. R. S. Rudrangi, H. S. J. Chellammal, and P. Sharma, "Luteolinencapsulated polymeric micelles for anti-inflammatory and neuroprotective applications: An in vivo study," *BioNanoSci.*, vol. 15, pp. 444–456, 2025, doi: 10.1007/s12668-025-02062-7.
- 13. A. Salama, N. Elsherbiny, H. F. Hetta, et al., "Curcumin-loaded gold nanoparticles with enhanced antibacterial efficacy and wound healing properties in diabetic rats," *Int. J. Pharm.*, vol. 666, p. 124761, 2024, doi: 10.1016/j.ijpharm.2024.124761.
- R. Tiwari, A. Patil, R. Verma, V. Deva, S. R. S. Rudrangi, M. R. Bhise, and A. Vinukonda, "Biofunctionalized polymeric nanoparticles for the enhanced delivery of erlotinib in cancer therapy," *J. Biomater. Sci. Polym. Ed.*, vol. 36, no. 7, pp. 817–842, 2025, doi: 10.1080/09205063.2024.2429328.
- 15. G. Tiwari, A. Shukla, A. Singh, and R. Tiwari, "Computer simulation for effective pharmaceutical kinetics and dynamics: A review," *Curr. Comput. Aided Drug Des.*, vol. 20, no. 4, pp. 325–340, 2024, doi: 10.2174/1573409919666230228104901.
- R. Tiwari, C. Khatri, L. K. Tyagi, and G. Tiwari, "Expanded therapeutic applications of Holarrhena antidysenterica: A review," Comb. Chem. High Throughput Screen., vol. 27, no. 9, pp. 1257–1275, 2024, doi: 10.2174/1386207326666230821102502.
- 17. N. Liu and H. Li, "Influence of phytosomal curcumin on anthropometric indices for nonalcoholic fatty liver disease: A meta-analysis," *Medicine (Baltimore).*, vol. 103, no. 52, p. e40538, 2024, doi: 10.1097/MD.00000000000040538.
- 18. G. Tiwari, R. Tiwari, and A. Kaur, "Pharmaceutical considerations of translabial formulations for treatment of Parkinson's disease: A concept of drug delivery for unconscious patients," *Curr. Drug Deliv.*, vol. 20, no. 8, pp. 1163–1175, 2023, doi: 10.2174/1567201819666220516161413.
- 19. R. Tiwari, G. Tiwari, S. Mishra, and V. Ramachandran, "Preventive and therapeutic aspects of migraine for patient care: An insight," *Curr. Mol. Pharmacol.*, vol. 16, no. 2, pp. 147–160, 2023, doi: 10.2174/1874467215666220211100256.

- R. Tiwari, J. R. Nandikola, M. K. D. Jothinathan, K. Shaik, G. Hemalatha, D. Prasad, and V. K. Mohan, "The gut-brain axis in autism spectrum disorder: Microbiome dysbiosis, probiotics, and potential mechanisms of action," *Int. J. Dev. Disabil.*, pp. 1–17, 2025, doi: 10.1080/20473869.2025.2462915.
- R. Tiwari, A. Paswan, G. Tiwari, V. J. S. Reddy, and M. K. Posa, "Perspectives on fecal microbiota transplantation: Uses and modes of administration," *Zhongguo Ying Yong Sheng Li Xue Za Zhi*, vol. 41, p. e20250014, 2025, doi: 10.62958/j.cjap.2025.014.
- 22. R. Tiwari, G. Tiwari, A. Lahiri, V. Ramachandran, and A. Rai, "Melittin: A natural peptide with expanded therapeutic applications," *Nat. Prod. J.*, vol. 12, no. 2, pp. 13–29, 2022, doi: 10.2174/2210315510999201210143035.
- 23. A. Patil, G. Singh, R. D. Dighe, D. Dev, B. A. Patel, S. Rudrangi, and G. Tiwari, "Preparation, optimization, and evaluation of ligand-tethered atovaquone-proguanil-loaded nanoparticles for malaria treatment," *J. Biomater. Sci. Polym. Ed.*, vol. 36, no. 6, pp. 711–742, 2024, doi: 10.1080/09205063.2024.2422704.
- N. G. R. Rao, P. Sethi, S. S. Deokar, R. Tiwari, H. N. Vishwas, and G. Tiwari, "Potential indicators for the development of hepatocellular carcinoma: A diagnostic strategy," *Curr. Top. Med. Chem.*, pp. 1–17, 2025, doi: 10.2174/0115680266349627250626142221.
- R. Tiwari, G. Tiwari, A. Singh, and N. Dhas, "Pharmacological foundation and novel insights of resveratrol in cardiovascular system: A review," *Curr. Cardiol. Rev.*, pp. 35–57, 2025, doi: 10.2174/011573403X343252250502045328.
- 26. G. Tiwari, M. Gupta, L. D. Devhare, and R. Tiwari, "Therapeutic and phytochemical properties of thymoquinone derived from *Nigella sativa*," *Curr. Drug Res. Rev.*, vol. 16, no. 2, pp. 145–156, 2024, doi: 10.2174/2589977515666230811092410.
- 27. G. Tiwari, A. Patil, P. Sethi, A. Agrawal, V. A. Ansari, M. K. Posa, and V. D. Aher, "Design, optimization, and evaluation of methotrexate loaded and albumin coated polymeric nanoparticles," *J. Biomater. Sci. Polym. Ed.*, vol. 35, no. 13, pp. 2068–2089, 2024, doi: 10.1080/09205063.2024.2366619.
- 28. P. Sethi, C. R. D., R. Borra, S. Vahora, A. Vashi, R. K. Mukherjee, B. Pavani, and G. Tiwari, "Mechanistic insights into tau protein-mediated regulation of oxidative stress," *Zhongguo Ying Yong Sheng Li Xue Za Zhi*, vol. 40, p. e20240028, 2024, doi: 10.62958/j.cjap.2024.028.
- 29. R. Tiwari, G. Tiwari, S. Sharma, and V. Ramachandran, "An exploration of herbal



- extracts loaded phyto-phospholipid complexes (phytosomes) against polycystic ovarian syndrome: Formulation considerations," *Pharm. Nanotechnol.*, vol. 11, no. 1, pp. 44–55, Jan. 2023, doi: 10.2174/2211738510666220919125434.
- 30. A. Kaur, R. Tiwari, G. Tiwari, and V. Ramachandran, "Resveratrol: A vital therapeutic agent with multiple health benefits," *Drug Res.* (*Stuttg*)., vol. 72, no. 1, pp. 5–17, Jan. 2022, doi: 10.1055/a-1555-2919.